# Micelle Formation of BAB Triblock Copolymers in Solvents That Preferentially Dissolve the A Block

**N. P. Balsara, M. Tirrell,* and T. P. Lodge**

*Department of Chemical Engineering and Materials Science and Department of Chemistry, University of Minnesota, Minneapolis, Minnesota 55455*

*Received April 4, 1990; Revised Manuscript Received October 13, 1990*

ABSTRACT: This study concerns the micellization of BAB triblock copolymers in solvents that preferentially dissolve the middle block. Spherical micelles in these systems would consist of a core containing B blocks, surrounded by loops of A blocks. The existence of this microstructure has not yet been established. In fact, the absence of micelles in these systems has been reported by a number of workers. Previous theoretical work indicates that the entropic penalty associated with the looping of the coronal block is substantial and precludes the possibility of micelle formation in these systems. Quasi-elastic light scattering measurements on solutions of poly(vinylpyridine)–polystyrene–poly(vinylpyridine) triblock copolymers in toluene, which is a selective solvent for the polystyrene block, indicate that these systems can form micelles. Furthermore, the diffusional characteristics of these micelles are similar to those of micelles formed by poly(vinylpyridine)–polystyrene diblock copolymers in toluene, implying a similarity in the overall architecture of the aggregate. It is found that the molecular weight of the middle block (polystyrene) plays a crucial role in determining the size and concentration of the micelles. Calculations presented here demonstrate that the previous analysis had overestimated the entropy of loop formation of the coronal block, and that micelle formation in these systems is indeed possible. However, the theory is only in partial agreement with experimental observations.

## Introduction

The ability of diblock and triblock copolymers to self-assemble into micelles, even in very dilute solutions, has been established for over two decades. Most studies have been concerned with AB and BAB block copolymers in solvents that are poor for the A block. The core of a micelle thus formed consists predominantly of A blocks and is surrounded by a corona of solvated B blocks extending into solution, as shown in Figure 1a.[1,2] The coronal chains are "tethered" at one end to the core–corona interface, while the other end is free to meander within the limits of the corona.

Relatively little is known about the effect of block copolymer architecture on micellization. Molecular architecture can impose constraints that force the resulting aggregates to adopt different morphologies. Triblock copolymers in solvents that preferentially dissolve the middle block provide an important example of such an effect. Figure 1b–d illustrates structures that might result from the self-assembly of these copolymers. In order to bring the two end blocks into the core of the micelle, the coronal block must form a loop. This results in an additional entropic penalty to the aggregating molecules. If this penalty is too large, it is conceivable that some of the copolymer chains in the micelle might elect to have one poorly solvated end block extending into solution, as shown in Figure 1c. Another possible mechanism for circumventing this penalty is through the formation of a branched structure, consisting of droplets of the poorly solvated blocked that are connected by strands of the well-solvated block, as shown in Figure 1d.[3]

The first observations on triblock copolymers with poorly solvated end blocks were reported in the pioneering work of Krause.[4] In fact, this study provided the first direct evidence of aggregation in block copolymer solutions in general. A triblock copolymer of poly(methyl methacrylate)–polystyrene–poly(methyl methacrylate) (PMMA–PS–PMMA) formed aggregates in triethyl benzene, which is a good solvent for PS but a nonsolvent for PMMA. However, the average mass of these micelles, as measured by light scattering, was distinctly lower than for micelles formed by the same polymer in acetone, which is a selective solvent for PMMA. This was attributed to the fact that acetone is a much stronger precipitant for PS than triethylbenzene is for PMMA. Possible structural differences between the aggregates formed by these two systems were not discussed. Tanaka et al.[5,6] also studied the solution properties of PMMA–PS–PMMA in *o*-xylene, a selective solvent for PS, and concluded from light scattering and

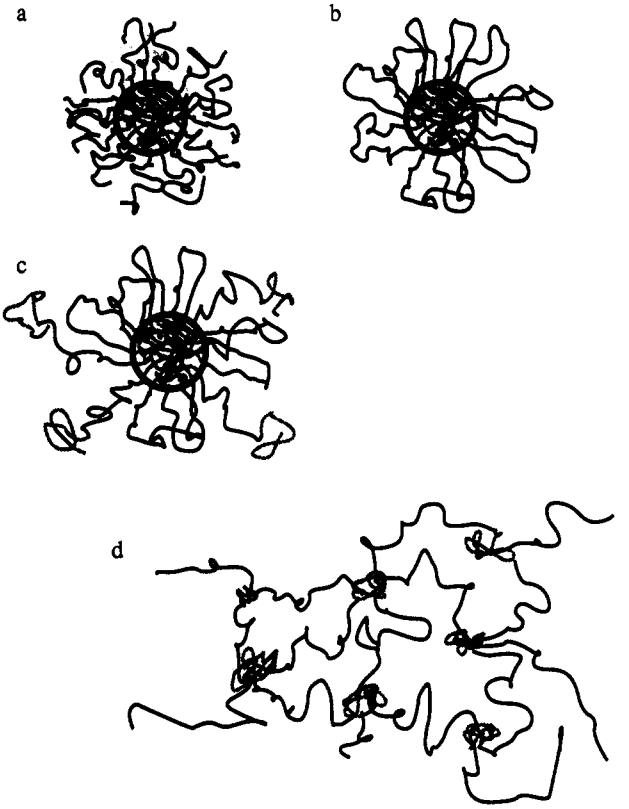


**Figure 1.** Possible structures of micelles formed by diblock and triblock copolymers in selective solvents. (a) Micelles formed by diblocks and triblocks in solvents selective toward the end blocks. (b–d) Possible structures formed by triblocks in solvents selective toward the middle block.

0024-9297/91/2224-1975$02.50/0 

viscometry that these molecules undergo intramolecular association of the PMMA blocks. There was no evidence of interchain micellization. Kotaka et al.[3] noted that PMMA–PS–PMMA did show evidence of aggregation in mixtures of toluene (a common solvent) and *p*-cumene (a selective solvent for PS). They also developed predictions for the particle scattering function of "conventional" micelles (Figure 1a,b) with transparent cores. An interesting feature of these measurements is that the solvent mixture and PMMA are almost isorefractive, and thus the PMMA should not contribute to the scattered intensity. While the measured scattering from solutions of PS–PMMA diblocks in the same solvent mixture agreed with the predictions, the data from the triblocks did not. It was evident that the triblocks did undergo some kind of intermolecular association, but the nature of the aggregate could not be determined. They speculated that these molecules might form a networklike structure, as illustrated in Figure 1d. Tang et al.[7,8] studied the properties of poly(2-vinylpyridine)–polystyrene–poly(2-vinylpyridine) (PVP–PS–PVP) in toluene, which is a selective solvent for PS, and observed no evidence of micellization under the conditions of their experiment.

In neither of the two papers cited above in which intermolecular aggregation was inferred[3,4] were the results definitive. For example, the polymer samples employed by Krause[4] were polydisperse and comprised molecules with widely differing compositions (7–72% styrene content). Similarly, the nature of the aggregation studied by Kotaka et al.[3] is difficult to assess, since the scattering patterns were anomalous and could not be analyzed within the framework of their theory. The use of solvent mixtures in this study also introduces an additional variable, the role of which is not immediately clear.

Theoretical aspects of possible micelle formation for triblock copolymers with poorly solvated end blocks were considered by ten Brinke and Hadziioannou.[9] They examined the formation of micelles with looped coronal blocks, as depicted in Figure 1b, and estimated that, under typical micellization conditions, the loss of entropy associated with the looping would be prohibitive and would therefore preclude the possibility of micelle formation. They noted that this was in agreement with the results of Tang et al.[7,8] and Tanaka et al.;[5,6] however, the authors did not address the data reported in refs 3 and 4.

The objective of the present work is to improve our understanding of these systems. In the first part of the paper we report quasi-elastic light scattering measurements on dilute solutions of triblock copolymers with poorly solvated end blocks in a single solvent; the system is PVP–PS–PVP in toluene. Our results demonstrate that these molecules are capable of spontaneous micellization. In the second section, we interpret the experimental data in terms of a simple model for micellization in these systems. In particular, we focus on the entropy of loop formation of the coronal block and find that the previous analysis[9] overestimated the associated entropic penalty and that micellization can be expected in these systems under some conditions.

## Experimental Section

**Materials.** The system chosen for this study was a set of four poly(2-vinylpyridine)–polystyrene–poly(2-vinylpyridine) (PVP–PS–PVP) triblock copolymers in toluene, a selective solvent for polystyrene. The numbers of monomer units in each of the blocks were determined to be 220–110–220, 250–230–250, 280–540–280, and 210–1240–210.[8] In addition, solutions of an 80–580 PVP–PS diblock copolymer was also examined. The polydispersities of the polymers were between 1.1 and 1.2. These polymers were synthesized by Tang and Hadziioannou.[8]

The samples used in the QELS experiments were prepared by filtering HPLC grade toluene into scattering cells containing a prescribed amount of polymer. A few selected samples were made by diluting stock solutions. No effect of sample preparation was found in the results. The samples were heated to 60 °C for about half an hour and then cooled slowly to the experimental temperature of 30 ± 0.1 °C. Varying the heating period from 5 min to 12 h had no effect on the measurements. A few samples were heated to 90 °C for 12 h and then cooled slowly back to 30 °C. This produced the same results as heating to 60 °C. However, solutions that had been at room temperature for an extended period of time and were heated directly to 30 °C gave erratic results. Further annealing of these samples produced the same reproducible results as heating directly to 60 °C. We believe on the evidence just described that the core of the micelle does not equilibrate readily at 30 °C. An open question, which may merit further study, is whether cooling from 60 °C leads to an equilibrium state at 30 °C. We can only assure that heating to 60 °C or higher, then cooling, leads to a reproducible state.

**Measurements and Data Analysis.** The solutions were examined by quasi-elastic light scattering (QELS). Details of the apparatus have been presented previously.[10] The time autocorrelation function of the scattered intensity was accumulated in the homodyne mode at five or more scattering angles by using a multisample time correlator (built by Brookhaven Instruments, model BI 2030). A distribution of sample times was used so that all modes of relaxation of the system were captured in a single experiment. The autocorrelation function of the scattered light, $g(\tau)$, is related to the intensity-weighted distribution of mobilities, $G(\Gamma)$, through an integral equation:[11]

$$g(\tau) = B[\{\int_0^\infty G(\Gamma) \exp(-\beta\tau)\, d\Gamma\}^2 + 1] \quad (1)$$

$B$ is the measured base line of the homodyne autocorrelation function. For a dilute system of particles undergoing Brownian motion, $\Gamma$ is related to their mutual diffusion coefficient, $D$.

$$D = \Gamma/q^2 \quad (2)$$

where $q$ is the scattering vector, defined as

$$q = \frac{4\pi n}{\lambda_0} \sin(\theta/2) \quad (3)$$

where $n$ is the refractive index of the solvent, $\lambda_0$ is the vacuum wavelength of the incident light beam (which was 514 nm in this case), and $\theta$ is the scattering angle.

The integral equation (1) was solved numerically by the experimentally measured autocorrelation function ($g(\tau)$) and base line ($B$), to obtain $G(\Gamma)$. This was accomplished with CONTIN, a software package developed by Provencher.[12] The inversion was obtained without imposing any constraints on the number of diffusive modes. Because of small but finite errors that occur in the measurement of $g(\tau)$, a large number of solutions can satisfy eq 1, within a prescribed set of error bounds. Consequently, CONTIN generates a number of solutions and selects one based on parsimony; i.e., the simplest solution that describes all of the features of the data is the most likely solution. All the data reported in this study are based on this, most probable solution.

**Experimental Results and Discussion.** Figure 2 illustrates typical results obtained for three different solutions at a scattering angle of 90°. In this figure, $w$ is the weight fraction of copolymer in solution. The distribution of mobilities of the solution containing the 220–110–220 triblock copolymer was unimodal (see Figure 2a). Furthermore, the mobility associated with this peak is slightly higher than that measured for a polystyrene molecule of the same total molecular weight as the triblock copolymer. Hence, it is in good agreement with the mobility we would expect for an unassociated triblock copolymer. (This point will be discussed further subsequently when the mobility of the triblock polymer is used to estimate its hydrodynamic radius.) This can be contrasted with the data obtained from the 80–580 diblock copolymer (Figure 2b). The measured mobility of this solution is peaked at a value that is lower by an order of magnitude than that expected of the unassociated chain. This is indicative of the fact that the copolymer molecules have self-assembled into relatively bulky aggregates, which exhibit a lower diffusion

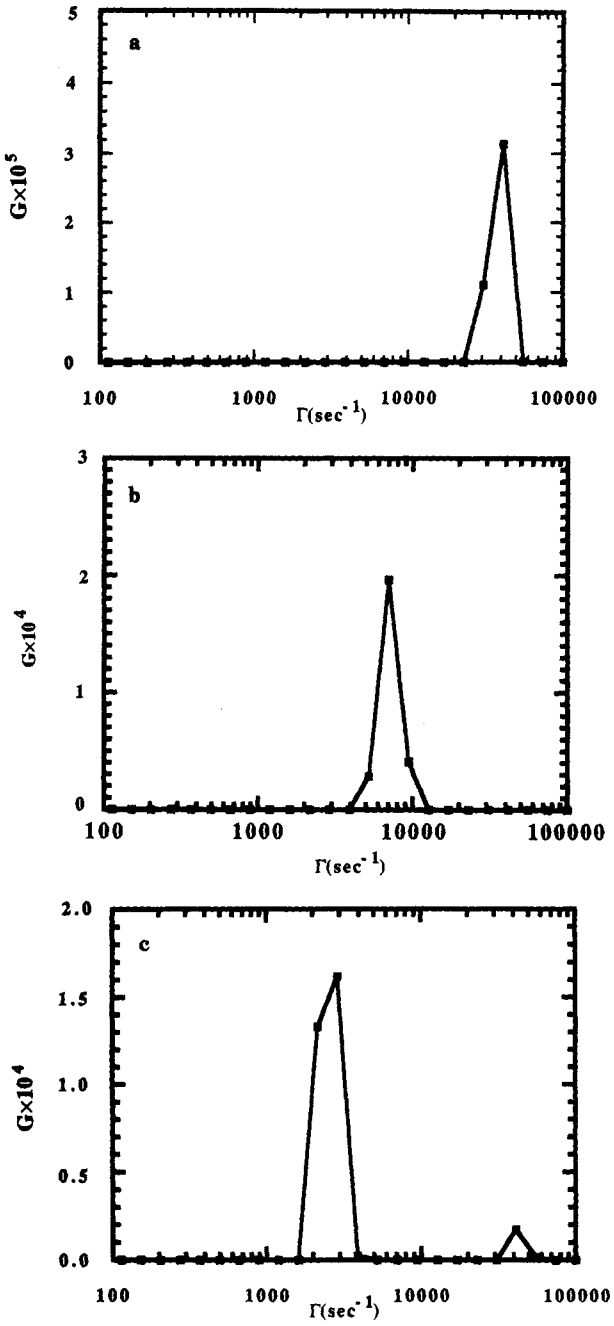


**Figure 2.** Typical intensity-weighted distributions of mobility obtained from solutions of the PVP–PS diblock and PVP–PS–PVP triblock copolymers in toluene. (a) 220–110–220, $w = 0.022$; (b) 80–580, $w = 0.001$; (c) 250–230–250, $w = 0.019$.

coefficient. In addition, independent static light scattering measurements from these solutions indicate that copolymer molecules form micelles containing roughly 25–30 chains.[8] It is widely accepted that block copolymer micelles coexist with unassociated molecules in solution. The absence of a peak corresponding to the unassociated molecule is presumably due to the fact that the signal is dominated by scattering from the micelle. Figure 2c shows data obtained from solutions of the 250–230–250 triblock. The distribution of mobilities is now bimodal with well-separated peaks. The peak with the higher mobility ($\Gamma \approx 40\,000$ s$^{-1}$) agrees well with the expected mobility of a single copolymer chain. The presence of the peak with the lower mobility ($\Gamma \approx 3000$ s$^{-1}$) indicates that some of the molecules have aggregated, presumably as a micelle. For most of the solutions examined, the mobilities were bimodal, with distinct peaks that could be identified with free chains and micelles. In a few cases, the signal was overwhelmingly dominated by one of the species.

The average mobility, $\Gamma_{av}$, of a given species is assumed to be the ratio of the first and zeroth moments of the corresponding

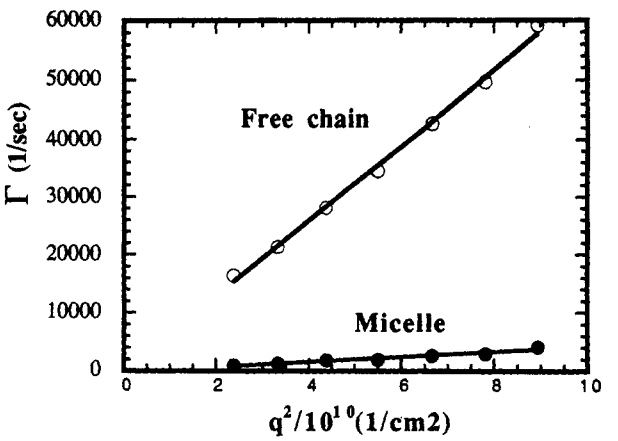


**Figure 3.** Typical dependence of $\Gamma_{av}$ on $q^2$, for micelles and free chains. 250–230–250 triblock in toluene, $w = 0.010$.

peak in the $G(\Gamma)$ versus $\Gamma$ curve. Figure 3 illustrates the typical angular dependence of the averaged mobilities of the unassociated chain and the aggregate. The data presented here is for a solution of the 250–230–250 triblock with $w = 0.010$. The averaged mobility of the micelles as well as the free chains was found to be linearly dependent on $q^2$. The mutual diffusion coefficients of the species were estimated from the slopes of the best linear fit to the $\Gamma_{av}$ versus $q^2$ data. The concentration dependence of the diffusion coefficients thus obtained is depicted in Figure 4; $w$ is the weight fraction of copolymer in solution. Figure 4a presents the data for the 220–110–220 triblock, which show no indication of aggregation up to a concentration of 3 wt %. Parts b, c, and d of Figure 4 show the dependence of the measured diffusion coefficient of the micelles and the free chains in solutions of the 250–230–250, 280–540–280, and 210–1240–210 triblock copolymers, respectively. In addition, Figure 4c contains the data obtained from the 80–580 diblock copolymer. The diffusional behavior of micelles formed by the 280–540–280 triblock is similar to that of the micelles obtained in solutions of the 80–580 diblock. This suggests a similarity in the overall architecture of the aggregates. The diffusion of a branched aggregate, for example, as shown in Figure 1d, would be much slower than that of a "conventional" micelle; these data show no evidence of such a slow diffusive mode. In addition, the internal modes of the branched structure might appear as $q$-independent relaxation modes. Again, our data are devoid of such features.

All of the results reported in this work are based on the most probable solution as selected by CONTIN. This corresponds to the result with the CONTIN smoothing parameter PROBI TO REJECT closest to 0.5. We found little variation in the results arising from PROBI TO REJECT values that were different from 0.5. For example, the 250–230–250 sample with $w = 0.010$ yielded five solutions with PROBI TO REJECT values from 0.404 to 0.997. All of them were bimodal. The mobility of the micellar peak varied from 2970 to 3260 s$^{-1}$ and that of the free chain from 49 700 to 67 200 s$^{-1}$.

The mutual diffusion coefficient of dilute solutions, $D$, can be expressed as

$$D = D_0(1 + \rho k_D w) \tag{4}$$

where $D_0$ is the self-diffusion coefficient of the particle and $\rho$ is the density of the solution. $k_D$ is composed of thermodynamic as well as frictional components. For a dilute solution of homopolymers, $k_D$ can be expressed as

$$k_D = 2A_2M_w - k_f \tag{5}$$

$A_2$ is the second virial coefficient that depends on intermolecular interactions, $M_w$ is the weight-average molecular weight of the polymer, and $k_f$ is related to the frictional drag that opposes the motion of the molecule. (For details, see ref 13.) The increase in friction owing to increasing polymer concentration is relatively unimportant in dilute solutions of homopolymers. The slope $k_D$ is strongly positive for polystyrene in toluene. Thus, negative values of $k_D$ are generally a signature of a poor solvent related to attractive interactions between the particles. As expected, the 220–110–220 molecules exhibit this behavior, due to the

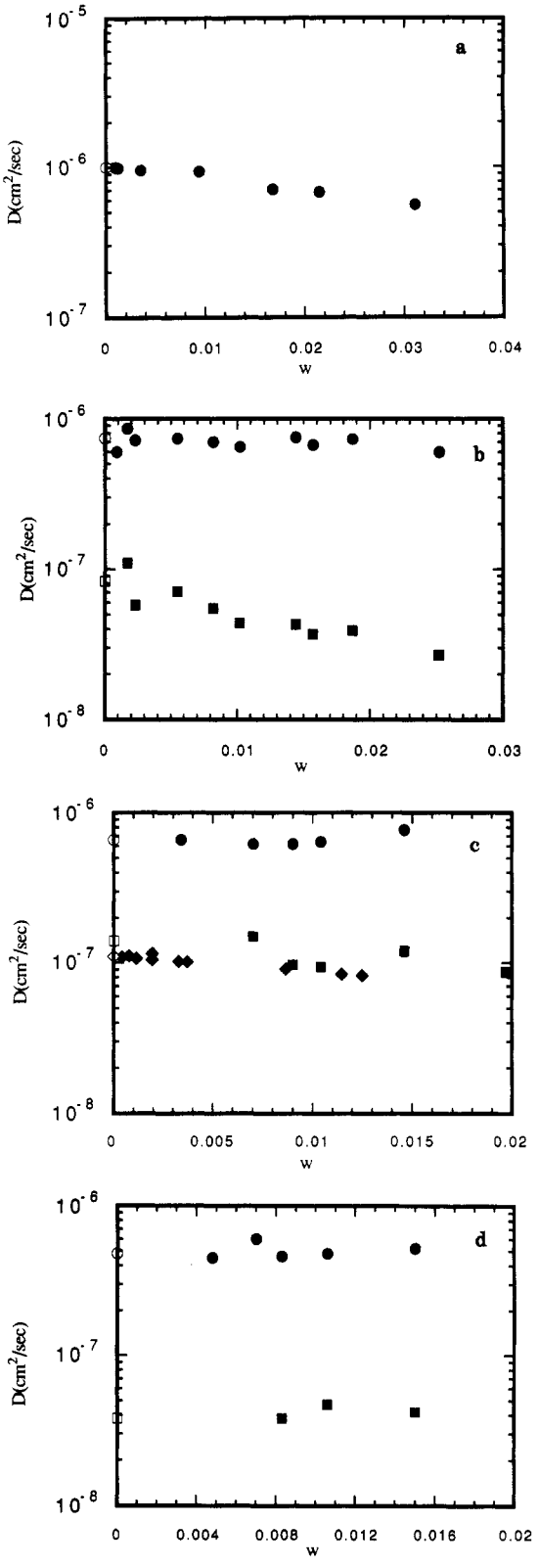


**Figure 4.** Dependence of the mutual diffusion coefficient of the micelles and free chains on $w$, the weight fraction of copolymer in solution for PVP–PS–PVP/toluene: (●) free chains; (■) triblock micelles; (♦) diblock micelles. The respective open symbols represent the self-diffusion coefficients of the micelles and the free chains, obtained by extrapolating the mutual diffusion coefficients to infinite dilution. (a) 220–110–220; (b) 250–230–250; (c) 280–540–280 and 80–580; (d) 210–1240–210.

presence of the poorly solvated PVP blocks (Figure 4a). In micellar solutions, one expects the interactions between micelles to be dominated by the composition of the coronae. Note that $D$ for the 250–230–250 triblocks decreases with increasing concentration. This could be interpreted as evidence that the poorly solvated PVP blocks are present in the corona, as shown in Figure 1c. However, the data from the 80–580 diblock also show a decrease in the diffusion coefficient with concentration. It is highly unlikely that the coronae of these micelles contain PVP. Thus, negative $k_D$ need not necessarily imply the presence of the poorly solvated block in the corona.

**Table I**
**Hydrodynamic Size of Micelles and Free Chains[a]**

Micelles

| block copolymer | $R_h$, nm |
|---|---|
| 220–110–220 | |
| 250–230–250 | 51 |
| 280–540–280 | 30 |
| 210–1240–210 | 108 |
| 80–580 | 38 |

Free Chains

| block copolymer | $R_h$ of triblock, nm | $R_h$ of PS of equal total mol wt, nm |
|---|---|---|
| 220–110–220 | 4.7 | 6.0 |
| 250–230–250 | 5.7 | 7.1 |
| 280–540–280 | 6.4 | 9.0 |
| 210–1240–210 | 10.8 | 11.4 |

[a] The size of the free chains is compared with literature values of the measured hydronamic size of polystyrene molecules[15] of the same total molecular weight as the triblocks. The hydrodynamic radii of the polystyrene chains in toluene were estimated by using the equation suggested by Huber et al.:[15] $D_0 = 3.40 \times 10^{-4} M_w^{-0.578}$ cm²/s.

An alternative explanation for this apparent discrepancy lies in the stretched nature of the coronal chains. The copolymer molecules in a micelle are in close proximity to each other, causing the coronal chains to assume highly stretched configurations. Direct force versus distance measurements on solvated, dense polymer brushes show that the repulsive forces between these layers are lower than those expected from the osmotic pressure exerted by unperturbed polymer chains at the same concentration.[14] The stretching of the chains increases the free energy of the layer, thereby decreasing the repulsive forces. One might thus expect the intermicelle interactions to be less repulsive than those between homopolymers in good solvents.

Another factor that could influence $D$ for the micelle is the increased frictional drag, due to its relatively large size. The decrease in $D$ with concentration also contains a contribution from the increase in friction with micelle concentration. It is thus difficult to interpret the diffusion data obtained from micellar solutions in terms of facts established on homopolymer solutions. A theory that specifically takes into account interactions between stretched spherical layers and the frictional drag on "hairy" objects would be necessary.

One can obtain the hydrodynamic radius ($R_h$) of each of the species from the diffusion data, using the Stokes–Einstein relationship.

$$R_h = kT/6\pi\eta_s D_0 \qquad (6)$$

$k$ is the Boltzmann constant, $T$ is the absolute temperature, and $\eta_s$ is the viscosity of the solvent. $D_0$ is the self-diffusion coefficient of the species, which is obtained by extrapolating the measured mutual diffusion coefficients to infinite dilution. The results of these extrapolations are shown as open symbols on the ordinates of Figure 4. The hydrodynamic radii of the micelles and the free chains thus obtained are tabulated in Table I. The dependence of the micellar size on the molecular weight of the PVP block will be compared to theoretical predictions in the following section. The measured sizes of the unassociated triblock molecules in toluene are compared to literature values for the hydrodynamic radius of homopolystyrene of the same total molecular weight as the triblock in toluene.[15] In all cases, we find that the triblocks have a smaller hydrodynamic size than the corresponding polystyrene molecule. This presumably reflects the fact that the triblock copolymers assume more compact configurations, due to the presence of the poorly solvated PVP blocks.

In addition, it is possible to obtain information regarding the relative abundance of micelles and free chains in equilibrium in

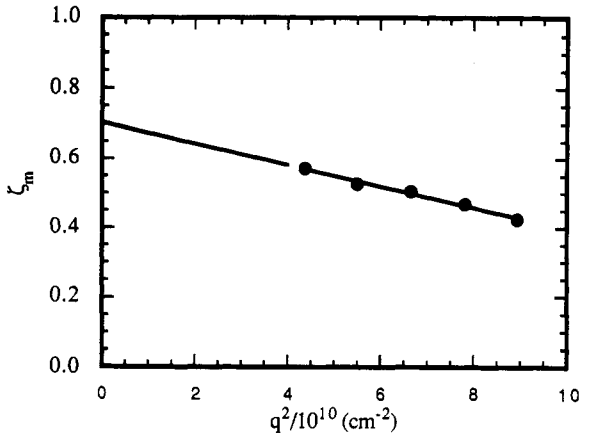


**Figure 5.** Typical dependence of $\zeta_m$ on $q^2$. 250–230–250 triblock, $w$ = 0.010.

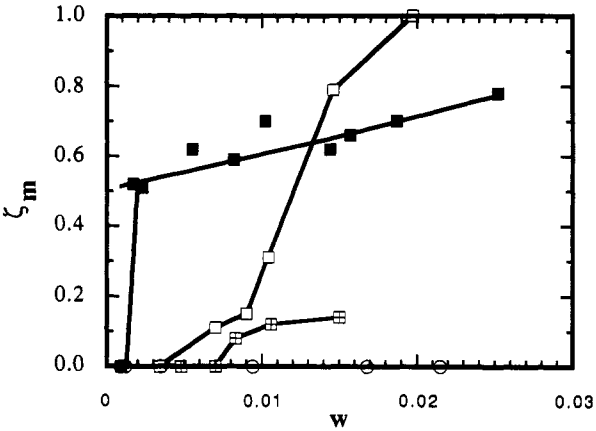


**Figure 6.** Dependence of $\zeta_m$ on $w$ for the triblock copolymer solutions. The symbols represent measured data. (○) 220–110–210; (■) 250–230–250; (□) 280–540–280; (□) 210–1240–210. The curves through each data set are meant to serve as a visual guide.

solution. The concentration of a given species is directly proportional to the area under the appropriate peak in the $G(\Gamma)$ versus $\Gamma$ curve (see Figure 2). In order to obtain the actual fraction of micellized copolymers, one needs to know the particle scattering function of the micelles and the free chains, which in turn requires knowledge of the structural details of the micelles and the configurations adopted by the free chains. Since this information is not available, we will only report results concerning the fraction of signal attributable to the micelle, $\zeta_m$.

$$\zeta_m = \text{area under micelle peak}/(\text{area under micelle peak} + \text{area under free chain peak}) \quad (7)$$

Figure 5 shows the typical dependence of $\zeta_m$ on the scattering vector. In all cases $\zeta_m$ was found to decrease linearly with $q^2$. The dependence of $\zeta_m$, extrapolated to zero scattering angle, on total polymer concentration for the various copolymers studied is depicted in Figure 6. We see that for the 250–230–250 triblock the signal from the micelle jumps from zero to about 50% at $w$ = 0.001 and then increases slowly to over the concentration range studied, to about 80%. The onset of micellization occurs at higher concentrations when $N_{PS}$ is increased to 540. At a concentration of 2%, we approach a state where the scattering from the micelles completely overwhelms the scattering from the free chains. Increasing the size of the middle block further to 1240 repeat units leads to a further delay in the onset of micellization and a dramatic decrease in $\zeta_m$. At the highest concentration studied, only 15% of the scattering was due to the micelle. This decrease in micelle concentration can be attributed to the increase in the entropic penalty associated with the looping of the relatively large coronal block. (This effect will be examined in detail in the Theoretical Section.)

Tang et al.[8] also studied some of the polymers used in this work. They performed total intensity light scattering measurements on the PVP–PS–PVP triblocks in toluene at concentrations less than 0.1 wt %. Their data show no evidence of micellization. This is consistent with our measurements, which show that the onset of micellization occurs at concentrations greater than 0.1 wt % for all the triblocks (see Figure 6).

## Theoretical Section

In this section we develop a theoretical basis for understanding the micellization of triblock copolymers in solvents that preferentially dissolve the middle block. The goal is to understand the origins of our experimental observations. This section is concerned with compact, spherical micelles, as shown in Figure 1b,c. The theory of branched aggregates (Figure 1d) is beyond the scope of the present work.

The nature of the equilibrium between micelles and free chains in block copolymer solutions has been studied by Leibler et al.[16] and by Noolandi and Hong.[17] The overall approach of both the treatments is similar. The work of Leibler et al. is more explicit in predictions for the onset of micellization; however, it is aimed at micellization in homopolymeric "solvents". Since the primary purpose of this section is to focus on the free energy effects arising from constraints due to molecular architecture, we choose to base our analysis on the theory of Leibler et al., recognizing that some effects due to swelling of the corona may need to be incorporated in an improved treatment. ten Brinke and Hadziioannou have developed a modification of this theory to study triblocks with poorly solvated end blocks.[9] They conclude, on the basis of their assumptions, that micelle formation of triblocks is unlikely. Use of the theory of Leibler et al. as a basis permits a direct comparison between predictions of the present work and that of ten Brinke and Hadziioannou. In particular, we show that the theory of ten Brinke and Hadziioannou overestimates the free energy penalty of loop formation and that micellization of triblocks is indeed possible.

**Free Energy of the Triblock Micelles.** We first consider the free energy of a micelle with looped coronal blocks, as depicted in Figure 1b. We assume that the triblock copolymers are monodisperse. The middle block consists of $N_A$ repeat units and the end blocks consist of $N_B$ repeat units each. $N$ (=$N_A + 2N_B$) is the total number of repeat units in each molecule. For simplicity, we assume that the monomer length of both blocks is $a$. Following Leibler et al.,[16] the solvent is assumed to consist of short homopolymer chains, with $N_H$ repeat units that are chemically identical with those of the middle block. This reduces the number of parameters in the model, because the enthalpy of mixing of the well-solvated block and the solvent is now identically zero.

We first consider micelles with looped coronal blocks. Figure 7 shows structural details of such a micelle. The free energy, $F_{micelle}$, is decomposed into contributions due to the formation of core, $F_{core}$, the corona, $F_{corona}$, and the interface between the core and the corona, $F_{int}$.

$$F_{micelle} = F_{core} + F_{corona} + F_{int} \quad (8)$$

The solvent is assumed to be excluded from the core, and thus $F_{core}$ is given by the deformation energy of the core blocks.

$$F_{core} = 2p\frac{3}{2}kT\left(\frac{R_B^2}{N_{Ba}^2} + \frac{N_B a^2}{R_B^2} - 2\right) \quad (9)$$

where $R_B$ is the radius of the core, $p$ is the number of chains per micelle, and $N_B a^2$ is assumed to be the unperturbed dimension of the core block. The free energy

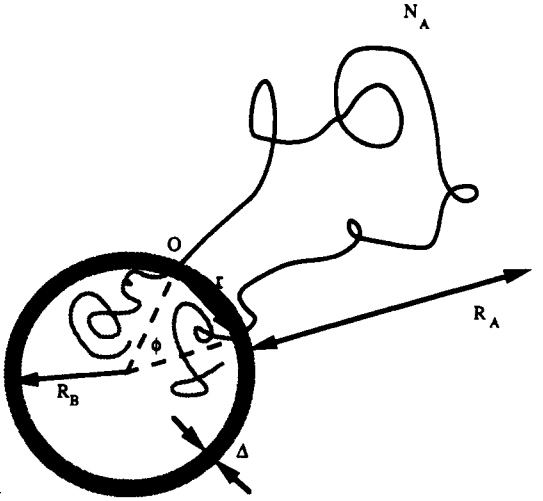


**Figure 7.** Details of the assumed structure of a triblock micelle. The cross-hatch area represents a spherical shell within the micelle.

of the corona is given by

$$F_{corona} = 2p\frac{3}{2}kT\left(\frac{2R_A^2}{N_A a^2} + \frac{N_A a^2}{2R_A^2} - 2\right) + \frac{pkTN_A(1-\eta)}{\eta N_H}\ln(1-\eta) + F_{loop} \quad (10)$$

where $R_A$ is the thickness of the corona and $\eta$ is the volume fraction of the A block in the corona. The first term in eq 10 represents the free energy of deformation of the corona block. The second term accounts for the entropy of mixing for the solvent and the block copolymer in the corona. The last term accounts for the loss of configurational entropy due to the constraint that both ends of the corona block must lie on the core–corona interface. In estimating the deformation energy of the core and corona blocks, we have used results valid for weakly perturbed Gaussian chains. We also remind the reader that there are no osmotic effects of the solvent in this modified melt model.

To estimate $F_{loop}$, we consider a chain emanating from a spherical shell of thickness $\Delta$, at a location O as shown in Figure 7. The spherical shell represents the core–corona interface. We assume that $w(\mathbf{r})$, the probability that the end-to-end vector of a chain of $N_A$ links is $\mathbf{r}$, is given by the Gaussian distribution

$$w(\mathbf{r}) = w(r) = \frac{\nu^3}{\pi^{3/2}}\exp(-\nu^2 r^2) \quad (11)$$

where $\nu^2 = 3/2N_A a^2$ and $r = |\mathbf{r}|$. This is clearly an approximation. The core of the micelle is impenetrable to coronal chains and this will distort the distribution $w(\mathbf{r})$. However, the level of approximation introduced here is the same as that used to calculate the deformation energies in eqs 9 and 10.

The fraction of chain configurations, $q$, that end up in the interface shell of thickness $\Delta$ is then given by

$$q = \int_{\phi=0}^{\phi=\pi} w(r) 2\pi \sin\phi R_B^2 \Delta \, d\phi \quad (12)$$

The configurational entropy associated with the formation of a micelle consisting of $p$ chains is given by

$$F_{loop} = -pkT\ln q \quad (13)$$

To a first approximation, the core–corona interface in the model resembles an interface between homopolymers A and B. These interfaces have been studied extensively and for highly incompatible pair of polymers, Helfand and Tagami have shown that the interfacial thickness, $\Delta$, is of the order of the monomer size, $a$.[18]

$$\Delta = \frac{2}{\sqrt{6}}a\chi^{-1/2} \quad (14)$$

where $\chi$ is the Flory–Huggins interaction parameter for the polymer pair. Then $F_{loop}$ can be evaluated from eqs 11–14.

$$F_{loop} - \frac{pkT}{2}\left\{\ln(\pi\chi N_A) - \ln\left[1 - \exp\left(-\frac{6R_B^2}{N_A a^2}\right)\right]^2\right\} \quad (15)$$

The first term in eq 15 represents the entropic loss associated with the return of a polymer chain to an infinite, flat interface with a thickness given eq 12. The second term corrects for the fact that the interface of interest is in fact a spherical shell. In most cases, this correction is negligible. The Gaussian distribution decays rapidly with $r$ and thus most of the configurations that return to the interface do so at very small $r$, wherein curvature effects are negligible.

In contrast, ten Brinke and Hadziioannou estimated $F_{loop}$ to be given by[9]

$$F_{loop} = \beta\left[\frac{3pkT}{2}\ln(N_A)\right] \quad (16)$$

The result in the bracket was obtained for the entropic loss associated with cyclization of a polymer chain.[9] Recognizing that the looping of the coronal block is not exactly a cyclization problem, they proposed a correction factor $\beta$, which they assumed would be close to unity. By comparison of eqs 15 and 16, it is obvious that in using the cyclization result ten Brinke and Hadziioannou have overestimated $F_{loop}$. To a first approximation, the correction factor, $\beta$, is $^1/_3$, not 1, and $F_{loop}$ is proportional to $\ln(\chi N_A)$, not $\ln(N_A)$. While these differences might appear to be relatively subtle, they have a substantial effect on the predictions of the theory.

In addition, the possibility of finding a structure such as that depicted in Figure 1c can be examined quantitatively. The free energy penalty associated with extending a poorly solvated core block into the corona is approximately $kT\chi N_B$ per chain. In comparison, the free energy of loop formation is approximately $kT\ln(\pi\chi N_A)/3$. Thus, for $N_A = 100$ and $\chi = 0.1$, which are typical values for these parameters, $N_B$ must be less than 10, for the two free energies to be comparable. This indicates that, except for triblocks with extremely small end blocks, the structure proposed in Figure 1b is more probable. The analysis that follows thus ignores the possibility of micelles with poorly solvated blocks in the corona. The free energy of the interface, $F_{int}$, is given by

$$F_{int} = 4\pi R_B^2\left[\frac{kT}{a^2}\left(\frac{\chi}{6}\right)^{1/2}\right] \quad (17)$$

The term in the brackets is the interfacial free energy between homopolymers A and B, as derived by Helfand and Tagami.[18]

This completes the description of the micelle. Although this model is developed for micellization of block copolymers in homopolymers, we feel it is reasonable to describe micellization in the presence of low molecular weight solvents. The equations that might cause concern are those related to the description of the core–corona interface. In the presence of solvents, this description is complicated, due to the three-component nature of the problem. In

order to make the problem tractable, several assumptions need to be made. In addition, it would introduce more parameters in the model. However, these more detailed calculations reveal that the interfacial thickness in these micelles is on the order of the monomer size, $a$.[17] Thus eq 14 is correct up to a prefactor. Difficulty also arises in calculating the free energy of the interface. One must account for the entropy of the solvent, which is now present in the interface. There seems to be no reliable way of taking this into account. Some workers have chosen to ignore these effects and have used the Helfand–Tagami results without modification for interfaces similar to those at issue here.[19,20] If we accept this and the uncertainty in the prefactors in eq 14, then this model is applicable to micellization in low molecular weight solvents. We thus feel that in spite of its simplicity, this model can be used to interpret the qualitative features of our data in light of the principal effect of interest here, that is, the ability of the coronal block to loop back into the core of the micelle. A quantitative description of micellization in solution will require the specification of more parameters and a better understanding of the interface.

**Free Energy of the System.** Let $\phi$ be the overall volume fraction occupied by the copolymer in the system. We ignore any volume changes that might occur on mixing the two components. If $\zeta$ is the fraction of copolymer chains that form micelles, the free energy density of the entire solution, $F_{total}$, can be expressed as

$$\frac{F_{total}}{kT} = \frac{\phi\zeta F_{micelle}}{N} + (1-\xi\phi\zeta)\left[\frac{\phi_1}{N}\ln\phi_1 + \frac{1-\phi_1}{N/\alpha}\ln(1-\phi_1) + \frac{\chi\phi_1}{1+f}\left(1-\frac{\phi_1}{1+f}\right)\right] - \left[\frac{\phi\zeta}{pN}\ln(\zeta\xi\phi) + \frac{1-\zeta\xi\phi}{\xi pN}\ln(1-\zeta\xi\phi)\right] \quad (18)$$

where $\alpha = N/N_H$ and $f = N_A/2N_B$. The first term is equal to the free energy of the micelles in solution, the second represents the free energy of mixing copolymer and solvent outside the micelles, and the last term accounts for the translational entropy of the micelles. $\phi_1$ is the volume fraction of copolymer chains outside the micelles and is given by

$$\phi_1 = \frac{\phi(1-\zeta)}{1-\zeta\xi\phi} \quad (19)$$

and

$$\xi = \frac{f+\eta}{\eta(1+f)} \quad (20)$$

$F_{total}$ can be expressed in terms of three independent variables, $p$, $\zeta$, and $\eta$, and requires the specification of model parameters $N_A$, $N_B$, $N_H$, $\chi$, and $\phi$. The expression for $F_{micelle}$ in terms of $p$, $\zeta$, and $\eta$ can be easily derived following Leibler et al.[16] and has been included in Appendix 1. The minimization of $F_{total}$ gives the equilibrium values of $p$, $\zeta$, and $\eta$. The minimization can be performed either by differentiating $F_{total}$ with respect to $p$, $\zeta$, and $\eta$ and solving the resulting algebraic equations numerically or by a direct minimization of $F_{total}$ using an optimization technique such as Powell's method.[21] Both methods yielded identical results.

**Theoretical Results and Their Relationship to Experiments.** Figure 8 compares the results of the present theory with those of ten Brinke and Hadziioannou[9] for $N_A = 200$, $N_B = 100$, $N_H = 40$, and $\chi = 0.1$. The theory of ten Brinke and Hadziioannou predicts that, for values of $\beta \geq 0.67$, the fraction of block copolymer chains

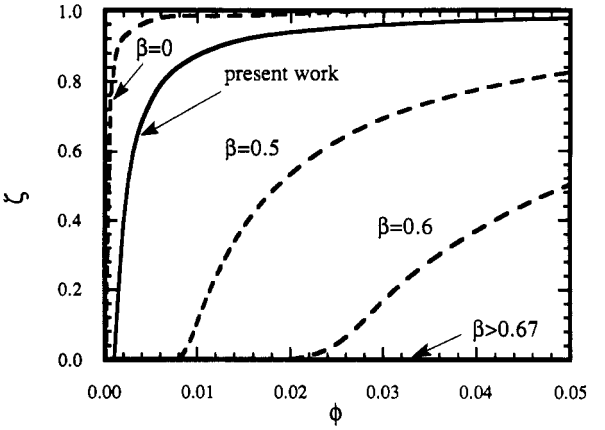


**Figure 8.** Theoretical predictions for the dependence of $\zeta$ on $\phi$. Dashed lines are the predictions of ten Brinke and Hadziioannou[9] for various values of $\beta$. The solid line represents results of the present work. $N_A = 200$; $N_B = 100$; $N_H = 40$; $\chi = 0.1$. (The number of copolymer chains per micelle, $p$, and the coronal concentration, $\eta$, depend weakly on $\phi$. For $\phi = 2.0 \times 10^{-3}$, $\zeta = 0.394$, $p = 38.3$, and $\eta = 0.189$. For $\phi = 2.0 \times 10^{-2}$, $\zeta = 0.938$, $p = 39.2$, and $\eta = 0.191$.)

in micellar form is negligibly small, while the present theory predicts strong micellizing tendencies for the same system. The overall features of the results of the present theory are similar to those of Leibler et al.[16] For a given set of parameters, $p$ and $\eta$ are only weakly dependent on $\phi$. For example, at $\phi = 0.0012$, $p = 37.6$, $\eta = 0.187$, and $\zeta = 0.053$, while at $\phi = 0.05$, $p = 39.4$, $\eta = 0.192$, and $\zeta = 0.977$. Since $p$ and $\eta$ determine the size of the micelle, the implication is that the size of the micelle is only weakly dependent on copolymer concentration. Another interesting feature of the triblock micelles is that, aside from the loops in the corona, they are predicted to be structurally similar to micelles formed by diblocks. Leibler et al.[16] found that for $N_H = 40$ and $\chi = 0.1$, diblocks with $N_A = 100$ and $N_B = 100$ formed micelles with $p \approx 79$ and $\eta \approx 0.19$ over a wide range of $\phi$ (0.01–0.1). Thus, triblock micelles resemble those formed by diblocks that are half the molecular weight of the triblock. Furthermore, it can be shown that the block copolymer composition plays a minor role in determining the size of the micelle, as long as the total molecular weight of the copolymer is kept fixed. The equations developed in the preceding section can be easily adapted to model the micellization of diblock copolymers. Of course, the free energy penalty associated with the looping of the coronal block is excluded from the calculations in that case. The appropriate equations for the micellization of diblock copolymers are presented in Appendix 2. The difference between the size of the micelles formed by a 30–170 diblock and a 89–120 diblock is only 10%. These arguments imply that micelles formed by triblock copolymers should be similar in size to those formed by diblock copolymers that are half the molecular weight of the triblock, regardless of the composition of the diblock. This is in agreement with the experimental observation that the measured size of the micelles formed by the 80–580 diblocks was similar to that of the 280–540–280 triblock.

The dependence of micellization on the molecular weight of the middle block is depicted in Figure 9. In these calculations, $\chi = 0.1$ and $N_B = 100$, while $N_A$ is varied from 50 to 600. We see that the onset of micellization occurs at higher copolymer concentrations, as the molecular weight of the middle block is increased. While the data obtained from the 250–230–250, 280–540–280, and 210–1240–210 solutions agree with this prediction, the 220–

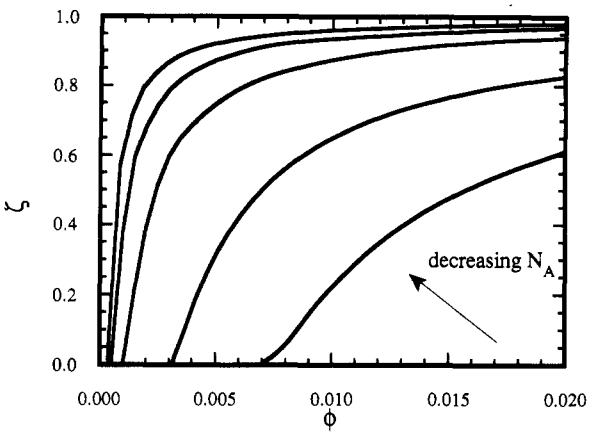


**Figure 9.** Theoretical predictions regarding the effect of the molecular weight of the middle block on micellization. $N_B$ = 100; $N_H$ = 40; $\chi$ = 0.1; $N_A$ = 50, 100, 200, 400, 600. (Typical values of $\zeta$, $p$, and $\eta$. $N_A$ = 50: For $\phi = 4.0 \times 10^{-4}$, $\zeta$ = 0.110, $p$ = 40.1, and $\eta$ = 0.141. For $\phi = 6.0 \times 10^{-3}$, $\zeta$ = 0.934, $p$ = 41.5, and $\eta$ = 0.143. $N_A$ = 200: For $\phi = 1.2 \times 10^{-3}$, $\zeta$ = 0.053, $p$ = 37.6, and $\eta$ = 0.187. For $\phi = 8.0 \times 10^{-3}$, $\zeta$ = 0.843, $p$ = 38.9, and $\eta$ = 0.190. $N_A$ = 600: For $\phi = 7.0 \times 10^{-3}$, $\zeta = 3.81 \times 10^{-3}$; $p$ = 31.9, and $\eta$ = 0.165. For $\phi = 2.0 \times 10^{-2}$, $\zeta$ = 0.611, $p$ = 33.5, and $\eta$ = 0.169.)

**Table II**
**Demonstration of the Validity of the Gaussian Approximation for Calculating the Looping Entropy, Even for Very Short Chains[a]**

| | $qa/\Delta$ | |
|---|---|---|
| $n$ | finite chain (eq A3.3) | Gaussian chain (eq A3.4) |
| 2 | 0.500 | 0.489 |
| 4 | 0.333 | 0.345 |
| 6 | 0.275 | 0.282 |
| 8 | 0.240 | 0.244 |
| 10 | 0.215 | 0.219 |
| 12 | 0.197 | 0.199 |
| 14 | 0.183 | 0.185 |
| 16 | 0.171 | 0.173 |
| 18 | 0.162 | 0.163 |
| 20 | 0.153 | 0.155 |
| 22 | 0.146 | 0.147 |
| 24 | 0.140 | 0.141 |

[a] $q$, the fraction of chain configurations that return to a flat interface of thickness $\Delta$, is given as a function of $n$, the number of repeat units in the chain. $a$ is the length of each repeat unit.

110–220 copolymer showed no sign of forming micelles. In contrast, the theory predicts that the triblocks with the smallest middle block should form micelles at the lowest concentrations. One might argue that the Gaussian distribution, which is strictly valid for infinite molecular weight polymers, is not appropriate for shorter middle blocks. However, a simple calculation proves that this is not the case. One can start with the distribution of end-to-end vectors for a polymer with a finite number of links and calculate the fraction of configurations that come back to the core–corona interface, $q$. The details of this calculation are given in Appendix 3. It turns out that the Gaussian approximation does remarkably well even for very short chains (see Table II). For example, $q$ obtained from the Gaussian approximation for a dimer ($N$ = 2) is within 2% of that obtained from the full calculation. This work is thus unable to provide any explanation for the lack of micelles in the case of the 220–110–220 copolymer.

The present theory predicts that increasing the total molecular weight of the triblock, without changing its composition, leads to increased micellization. This is illustrated in Figure 10, where the fraction of micelles formed at a fixed overall copolymer concentration of 0.05

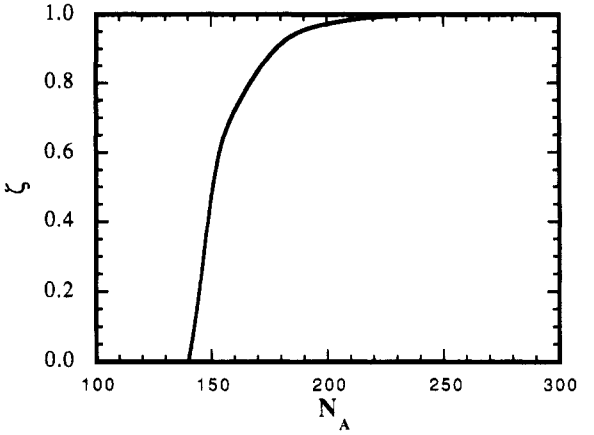


**Figure 10.** Theoretical predictions regarding the effect of the total molecular weight of triblock copolymers on micellization. $N_A = 2N_B$; $N_H$ = 40; $\chi$ = 0.1; $\phi$ = 0.05. (Typical values of $\zeta$, $p$, and $\eta$: For $N_A$ = 150, $\zeta$ = 0.584, $p$ = 32.3, and $\eta$ = 0.190. For $N_A$ = 200, $\zeta$ = 0.977, $p$ = 39.5, and $\eta$ = 0.192.)

**Table III**
**Theoretical Predictions for Micelle Formation in Triblock Copolymers:[a] $\chi$ = 0.6; $N_H$ = 2**

| triblock copolymer | $\phi_{cmc}$ ($\phi$ at $\zeta$ = 0.5) | $p^b$ | $R$,[c] nm |
|---|---|---|---|
| 250–100–250 | $2.7 \times 10^{-9}$ | 137 | 19 |
| 250–250–250 | $2.6 \times 10^{-7}$ | 93 | 22 |
| 250–500–250 | $2.5 \times 10^{-3}$ | 65 | 27 |
| 250–1200–250 | $1.4 \times 10^{-1}$ | 43 | 38 |

[a] In small molecule solvents; $N_A$ and $N_B$ as indicated. Parameters are chosen so as to model the PVP–PS–PVP/toluene system. [b] Chains per micelle. [c] Radius of micelle.

is shown to increase monotonically as $N$ is increased. The triblocks considered here are such that $N_A = 2N_B$. There are two opposing tendencies that arise as $N$ is increased. The increase in the molecular weight of the poorly solvated block tends to favor micelle formation, while the increase in the molecular weight of the well-solvated block hinders micellization, due to the entropy of loop formation. The present theory predicts that the former tendency dominates, leading to an increase in micellization with increasing $N$. Whether this prediction agrees with experiments or not remains to be seen.

Although this model is best suited for describing the micellization of block copolymers in the presence of homopolymers, we have argued that it should qualitatively describe micellization of block copolymers in small-molecule solvents. In order to stimulate the PVP–PS–PVP/toluene system, the following model parameters were chosen: $N_B$ = 250, $N_H$ = 2, and $\chi$ = 0.6. $N_A$ was varied from 100 to 1200. The theoretical predictions for these systems are summarized in Table III. We define the critical micelle concentration (cmc) as the value of $\phi$ at which $\zeta$ = 0.5. Our calculations show that, whereas the onset of micellization is very sensitive to the chosen values of $N_H$ and $\chi$, the radius of the micelle, $R$, is not. For example, changing $N_H$ from 2.0 to 1.9 shifts the predicted onset of micellization by 4 orders of magnitude; the cmc changes from $2.7 \times 10^{-9}$ to $1.9 \times 10^{-4}$. In light of this extreme sensitivity, quantitative comparisons between theory and experiment are difficult. However, the calculated size of the micelles are relatively insensitive to changes in $\chi$ and $N_H$ and thus can be compared with the measured quantities. We find that the measured size of the micelles formed by the 280–540–280 copolymer agrees quantitatively with the theoretical predictions. However, the theory underpredicts the size of the micelles formed by

the 250–230–250 and 210–1240–210 copolymers. This could be due to the fact that the aggregates formed by these weakly micellizing systems might be loose aggregates, like those found at the onset of micellization in diblock copolymers.[22] It should be noted that the solutions of both 250–230–250 and 210–1240–210 copolymers showed evidence of the existence of free chains, even at the highest concentrations studied. It is also possible that the many simplifications employed in this treatment are responsible for this discrepancy. Finally, one should realize that we are comparing a predicted structural quantity, $R$, with a measured dynamic quantity, $R_h$.

## Concluding Remarks

The main conclusion of this work is that triblock copolymers can form micelles in solvents that preferentially dissolve the middle block. Our experimental observations on the PVP–PS–PVP/toluene system demonstrate this. The diffusional behavior of these micelles is similar to that of "conventional" micelles formed by diblock copolymers. We see no evidence of the formation of branched structures in the range of concentrations and molecular weights studied. However, it is entirely possible that, at higher concentrations, the compact micelles might give way to networklike aggregates. Furthermore, micelles formed by triblocks were found to be similar in size to those formed by diblocks that were half the molecular weight of the triblocks, indicating a similarity in the overall structure of the micelle. This is in agreement with theoretical predictions.

However, there are important differences between the micellization of diblocks and triblocks. The onset of micellization occurs at higher concentrations in triblocks. While the onset of micellization in the 80–580 solutions occurred at concentrations lower than $w = 0.0004$, which is the lower limit of instrumental resolution, the triblocks studied in this work formed micelles at about $w = 0.005$. Unlike the diblock solutions, where the QELS signals were dominated by the micelles, the triblock solutions exhibited two resolvable diffusive modes, one associated with the free chains, the other with micelles.

Experiments also reveal that the molecular weight of the middle block plays a crucial role in determining the micellization characteristics of the system. Triblock copolymers with very small middle blocks formed nonmicellar solutions. When the molecular weight of the middle block was increased to the point that the blocks were comparable in size, we see the onset of micellization. The copolymer concentration at the onset of micellization increased with the molecular weight of the middle block. The triblock with equal composition of PVP and PS was the only one that showed signs of complete micellization. By complete micellization, we mean that the measured signal was completely dominated by micelles and that the free chain motion was unresolvable.

The results of our theoretical treatment show that the entropic penalty associated with the looping of the coronal block is not as severe as estimated by ten Brinke and Hadziioannou.[9] Our theory shows that the driving forces typical of micellizing systems are capable of overcoming this entropic barrier. In addition, we were able to show that, in most cases, micelles with looped coronae are thermodynamically more stable than micelles with poorly solvated blocks in the corona. Finally, the theoretical predictions regarding micelle formation are strongly dependent on the molecular weight of the middle block. However, the predicted dependence was only in partial agreement with experimental observations. While the theory was able to explain the delay in the onset of micellization as the number of repeat units in the middle block was increased from 230 to 1240, it was unable to explain why the triblock with the smallest middle block did not show signs of micellization. The theoretical predictions for the size of the micelles agreed well with the measured hydrodynamic size of the 280–540–280 copolymer. However, the measured sizes of the micelles formed by the 250–230–250 and 210–1240–210 copolymers were substantially larger than the theoretical predictions. It seems as if the theory is capable of describing the triblock copolymers that have strong micellizing tendencies. In the present case, this happened to be the polymer with equal composition ($N_A \approx 2N_B$).

**Acknowledgment.** It is a pleasure to acknowledge Dr. Sanjay Patel of AT&T Bell Laboratories for his help with the computations, and the Shell Companies Foundation and the Center for Interfacial Engineering for financial support. This work would not have been possible without the cooperation of Georges Hadziioannou and Wing Tang, who provided us with the materials we studied. M.T. acknowledges with thanks the Olaf A. Hougen Visiting Professorship in Chemical Engineering at the University of Wisconsin, Madison, for providing the environment for the completion of this manuscript.

## Appendix 1. Expression for $F_{micelle}$ in Terms of $p$, $\zeta$, and $\eta$

$F_{micelle}$ can be expressed in terms of $p$, $\zeta$, and $\eta$ by recognizing that

$$2pN_B a^3 = \frac{4}{3}\pi R_B^3 \tag{A1.1}$$

and

$$pN_A a^3 = \frac{4}{3}\pi\{(R_A + R_B)^3 - R_B^3\}\eta \tag{A1.2}$$

See ref 16 for details. Equations 8–10, 15, A1.1, and A1.2 give

$$\frac{F_{micelle}}{pkT} = \frac{4\pi}{\sqrt{6}}\left(\frac{3}{2\pi}\right)^{2/3} N_B^{2/3} p^{-1/3}\chi^{1/2} + 3\left(\frac{3}{2\pi}\right)^{2/3} N_B^{-1/3} p^{2/3}[1 + C(\eta)] + 3\left(\frac{2\pi}{3}\right)^{2/3} N_B^{1/3} p^{-2/3} \times \left[1 + \frac{1}{C(\eta)}\right] + \frac{\alpha f(1-\eta)}{\eta(1+f)}\ln(1-\eta) + \frac{1}{2}\ln(\pi\chi N_B) - \ln\left[1 - \exp\left\{-\frac{3}{2}\left(\frac{3}{2\pi}\right)^{2/3} N_B^{-1/3} p^{2/3} f^{-1}\right\}\right] - 12 \tag{A1.3}$$

$C(\eta)$ is given by

$$C(\eta) = \frac{1}{f}\{(1 + f/\eta)^{1/3} - 1\}^2 \tag{A1.4}$$

## Appendix 2. Micellization of Diblock Copolymers

The equations developed by Leibler and co-workers[16] were explicitly for diblocks with $N_A = N_B$, although their ideas are valid for block copolymers of arbitrary composition. The equations for $N_A \neq N_B$ were derived by Munch and Gast.[20] However, their reported numerical results appear to be in error. The equations that govern the micellization of diblock copolymers of arbitrary composition are given below. Aside from minor typographical errors that appear in eq 6 of ref 20, they are mathematically

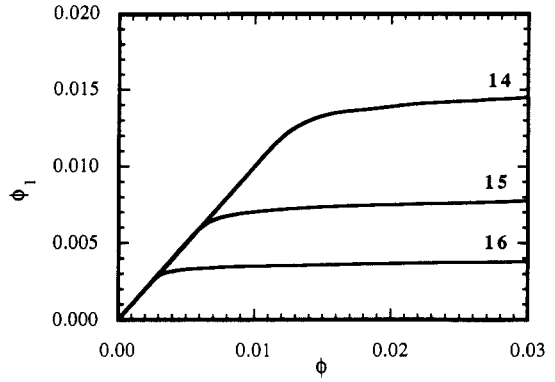


**Figure 11.** Concentration of free diblock copolymer outside micelles, $\phi_1$, as a function of the overall copolymer concentration, $\phi$. $N = 200$; $N_H = 4$; $f = 10$; $\chi N_B = 14, 15, 16$.

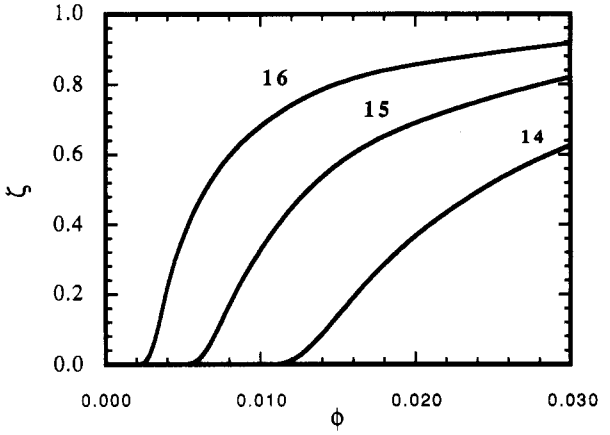


**Figure 12.** Fraction of micellized copolymer chains, $\zeta$, as a function of overall copolymer concentration, $\phi$. $N = 200$; $N_H = 4$; $f = 10$; $\chi N_B = 14, 15, 16$. (Typical values of $\zeta$, $p$, and $\eta$: For $\chi N_B = 14$ and $\phi = 0.03$, $\zeta = 0.626$, $p = 19.6$, and $\eta = 0.076$. For $\chi N_B = 15$ and $\phi = 0.03$, $\zeta = 0.821$, $p = 19.7$, and $\eta = 0.074$. For $\chi N_B = 16$ and $\phi = 0.03$, $\zeta = 0.917$, $p = 20.0$, and $\eta = 0.073$.)

identical with those of Munch and Gast.

$$\frac{F_{total}}{kT} = \frac{\phi\zeta F_{micelle}}{N} + (1 - \xi\phi\zeta)\left[\frac{\phi_1}{N}\ln\phi_1 + \frac{1-\phi_1}{N/\alpha}\times \ln(1-\phi_1) + \frac{\chi\phi_1}{1+f}\left(1 - \frac{\phi_1}{1+f}\right)\right] - \left[\frac{\phi\zeta}{pN}\ln(\zeta\xi\phi) + \frac{1-\zeta\xi\phi}{\xi pN}\ln(1-\zeta\xi\phi)\right] \quad \text{(A2.1)}$$

$$\frac{F_{micelle}}{pkT} = \frac{4\pi}{\sqrt{6}}\left(\frac{3}{4\pi}\right)^{2/3} N_B^{2/3} p^{-1/3}\chi^{1/2} + \frac{3}{2}\left(\frac{3}{4\pi}\right)^{2/3} N_B^{-1/3} p^{2/3}[1 + C(\eta)] + \frac{3}{2}\left(\frac{4\pi}{3}\right)^{2/3} N_B^{1/3} p^{-2/3}\left[1 + \frac{1}{C(\eta)}\right] + \frac{\alpha f(1-\eta)}{\eta(1+f)}\times \ln(1-\eta) - 6 \quad \text{(A2.2)}$$

where $f = N_A/N_B$. All other variables have the same definitions as the triblock treatment.

The results of the minimization of $F_{total}$ for the some of the parameters used by Munch and Gast ($N = 200$, $f = 10$, and $N_H = 4$) are given in Figures 11 and 12. These results differ numerically from the results of Munch and Gast. For example, the number of chains per micelle, $p$, lies between 18 and 20 for $\chi N_B$ between 14 and 16. Figure 3 in ref 20 indicates that $p$ increases from 20 to 35 when

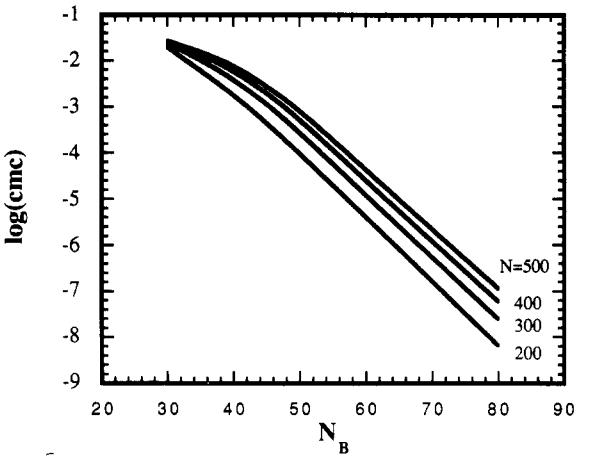


**Figure 13.** Dependence of the critical micelle concentration on the number of repeat units in the poorly solvated block, $N_B$. $N_H = 4$; $\chi = 0.6$; $N$ as indicated.

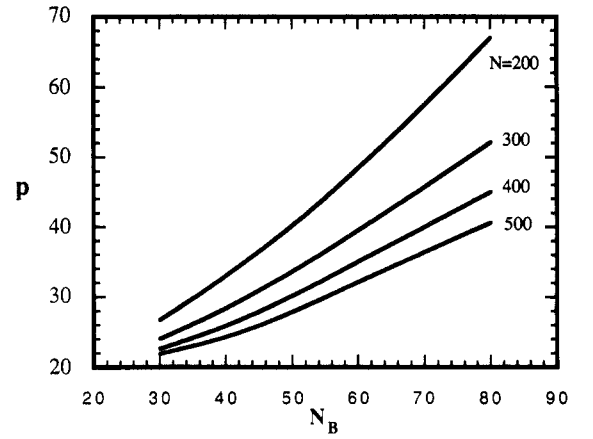


**Figure 14.** Number of chains per micelle, $p$, as a function of the number of repeat units in the poorly solvated block, $N_B$. $N_H = 4$; $\chi = 0.6$; $N$ as indicated.

$\chi N_B$ is changed from 14 to 16. Similarly, the onset points of micellization for the same systems differ substantially from the results reported here (Figure 11). The parameters used by Munch and Gast were chosen to model micelle formation of diblocks in small-molecule solvents. Their prediction that the onset of micellization occurs at concentrations greater than 10% for these systems is in disagreement with experimental evidence. Most diblocks form micelles at much lower concentrations. In fact, block copolymer micelles begin to organize themselves into macrolattices at these concentrations.[23] This suggests that there are numerical, though we believe no conceptual, errors in the results of Munch and Gast. Our calculations show that the model of Leibler et al., as suggested by Munch and Gast, does give reasonable results for micellization in solvents even though the applicability of some of the assumptions may be questioned.

The dependence of $\phi_1$ and $\zeta$ on $\phi$ (Figures 11 and 12, respectively) is qualitatively similar to the results presented by Leibler et al. The transition from a molecular solution ($\zeta \approx 0$) to a micellar solution ($\zeta \approx 1$) is gradual for polymeric surfactants and thus the definition of a critical micelle concentration (cmc) is somewhat arbitrary. We have defined the cmc as the concentration ($\phi$) at which half the copolymer chains are in micellar form ($\zeta = 0.5$). The effects of block copolymer composition on micellization are summarized in Figures 12–14. Because the equations developed by Leibler et al. were applicable to symmetric diblock copolymers only, these effects were not

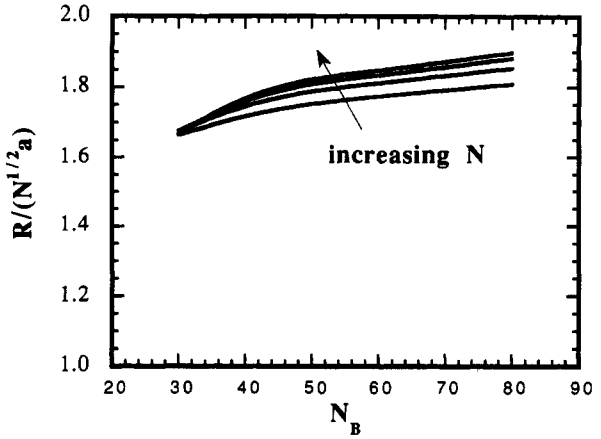


**Figure 15.** Scaled radius of the micelle, $R/Na^{1/2}$, as a function of the number of repeat units in the poorly solvated block, $N_B$ ($R = R_A + R_B$). $N_H = 4$; $\chi = 0.6$; $N = 200, 300, 400, 500$.

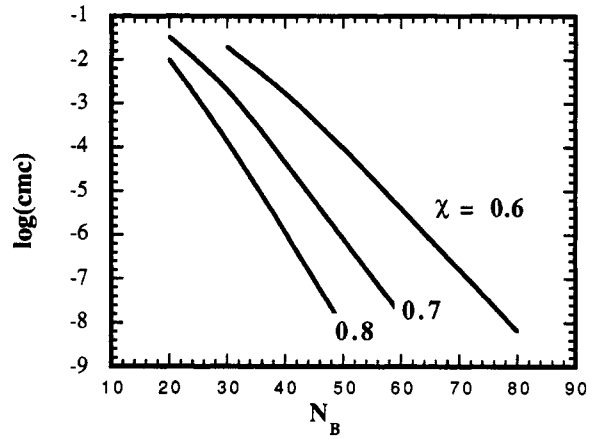


**Figure 16.** Dependence of the critical micelle concentration on the number of repeat units in the poorly solvated block, $N_B$, for various interaction parameters, $\chi$. $N = 200$; $N_H = 4$, $\chi$ as indicated. (Typical values of $\zeta$, $p$, and $\eta$ for $N_B = 40$: For $\chi = 0.8$ and $\phi = 1.12 \times 10^{-6}$, $\zeta = 0.499$, $p = 33.9$, and $\eta = 0.091$. For $\chi = 0.7$ and $\phi = 4.5 \times 10^{-5}$, $\zeta = 0.498$, $p = 33.5$, and $\eta = 0.091$. For $\chi = 0.6$ and $\phi = 1.7 \times 10^{-3}$, $\zeta = 0.499$, $p = 33.0$, and $\eta = 0.090$.)

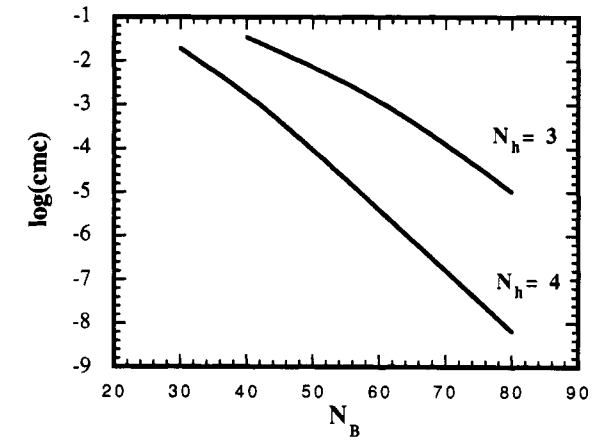


**Figure 17.** Dependence of the critical micelle concentration on the number of repeat units in the poorly solvated block, $N_B$, for $N_H = 3$ and 4. $N = 200$; $\chi = 0.6$. (Typical values of $\zeta$, $p$, and $\eta$ for $N_B = 40$: For $N_h = 3$ and $\phi = 3.45 \times 10^{-2}$, $\zeta = 0.504$, $p = 32.5$, and $\eta = 0.083$. For $N_H = 4$ and $\phi = 1.7 \times 10^{-3}$, $\zeta = 0.499$, $p = 33.0$, and $\eta = 0.090$.)

included in their treatment. As is evident from Figure 12, the onset of micellization is dramatically affected by the composition of the block copolymer. In fact, for a given molecular weight of the copolymer, $N$, the cmc decreases exponentially with the size of the poorly solvated block, $N_B$. The size of the well-solvated block, $N_A$, plays a relatively minor role in determining the cmc of the system. This is especially true for highly asymmetric diblocks; the cmc for a 20–180 copolymer is almost identical with that of a 20–480 copolymer. In contrast, altering the size of the poorly solvated block has a profound effect on the cmc; the cmc of a 80–120 copolymer is 8 orders of magnitude lower than that for a 20–180 copolymer.

The characteristics of the micelles formed at the cmc for the systems discussed in the preceeding paragraph are illustrated in Figures 13 and 14. The number of chains per micelle increases monotonically as we increase either $N_A$ or $N_B$. However, the radius of the micelle, $R$, when scaled by the unperturbed dimension of the copolymer chains, $N^{1/2}a$, is fairly insensitive to $N_A$ and $N_B$.

In the above discussion, $\chi$ and $N_H$ were held fixed at 0.6 and 4, respectively. Figures 15 and 16 illustrate the effect of changing these parameters. In these calculations, $N$ is held fixed at 200. The cmc decreases rather dramatically with increasing $\chi$ and $N_H$.

## Appendix 3. The Looping Entropy of a Chain with a Finite Number of Links

This appendix is concerned with the calculation of the entropic penalty associated with the looping of the coronal chain using the exact distribution function of end-to-end vectors for a freely jointed polymer chain with a finite number of segments, $n$. This distribution function is given by[24]

$$w(r) = \frac{1}{2^{n+1}(n-2)!\pi a^2 r} \sum_{k=0}^{k=\frac{n-r/a}{2}} (-1)^k \binom{n}{k} (n - 2k - r/a)^{n-2} \tag{A3.1}$$

In the Theoretical Section of this work we showed that the entropic penalty of looping a Gaussian coronal chain can be well approximated by considering the return of the chain to a flat interface. This approximation is better suited for shorter chains because the distribution function will decay even more rapidly. Since our interest here is primarily in short chains, we consider the return of chains with a finite number of links to flat interfaces with thickness $\Delta$. The fraction of configurations that return to the interface, $q$, is given by

$$q = \int_0^{na} w(r) \Delta 2\pi r \, dr \tag{A3.2}$$

The solution that follows applies for even $n$, although the treatment can easily be adapted for odd $n$. It is convenient to integrate over intervals of $ma \le r \le (m + 2)a$, where $m$ is an even integer between 0 and $(n - 2)$. On carrying out the integration, one gets

$$q = \left(\frac{\Delta}{a}\right) \frac{1}{2^n(n-2)!} \times \sum_{\substack{m=2 \\ (m \text{ even})}}^{n} \sum_{k=0}^{k=\frac{n-m}{2}} (-1)^k \binom{n}{k} \left\{ \frac{(n - 2k - m + 2)^{n-1}}{n-1} - \frac{(n - 2k - m)^{n-1}}{n-1} \right\} \tag{A3.3}$$

In comparison, $q$ for a Gaussian chain is given by

$$q = \frac{\Delta}{a}\frac{1}{n^{1/2}}\left(\frac{3}{2\pi}\right)^{1/2} \quad \text{(A3.4)}$$

Table II compares $qa/\Delta$ for a random chain with finite links with that for a Gaussian chain. Even for $n = 2$, the Gaussian approximation does well.

## References and Notes


(1) Tuzar, Z.; Kratochvil, P. *Adv. Colloid Interface Sci.* **1976**, *6*, 201.
(2) Price, C. *Development of Block Copolymers*; Goodman, I., Ed.; Applied Science: Long, 1982; Vol. I, p 39.
(3) Kotaka, T.; Tanaka, T.; Hattori, M.; Inagaki, H. *Macromolecules*, **1978**, *11*, 138.
(4) Krause, S. *J. Phys. Chem.* **1964**, *68*, 1948.
(5) Tanaka, T.; Kotaka, T.; Inagaki, H. *Polym. J.* **1972**, *3*, 327.
(6) Tanaka, T.; Kotaka, T.; Inagaki, H. *Polym. J.* **1972**, *3*, 338.
(7) Tang, W. T.; Hadziioannou, G.; Cotts, P. M.; Smith, B. A.; Frank, C. W. *Polym. Prepr. (Am. Chem. Soc., Div. Polym. Chem.)* **1986**, *27* (2), 107.
(8) Tang, W. T. Ph.D. Thesis, Stanford University, 1987.
(9) ten Brinke, G.; Hadziioannou, G. *Macromolecules* **1987**, *20*, 486.
(10) Lodge, T. P.; Markland, P. *Polymer* **1987**, *28*, 1377.
(11) Koppel, D. E. *J. Chem. Phys.* **1972**, *57*, 4814.
(12) Provencher, S. *Makromol. Chem.* **1979**, *180*, 201.
(13) Berne, B. J.; Pecora, R. *Dynamic Light Scattering*; Wiley: New York, 1976; p 334.
(14) Patel, S. S.; Tirrell, M. *Annu. Rev. Phys. Chem.* **1989**, *40*, 597.
(15) Huber, K.; Bantle, S.; Lutz, P.; Burchard, W. *Macromolecules* **1985**, *18*, 1461.
(16) Leibler, L.; Orland, H.; Wheeler, J. C. *J. Chem. Phys.* **1983**, *79*, 3550.
(17) Noolandi, J.; Hong, K. M. *Macromolecules* **1983**, *16*, 1443.
(18) Helfand, E.; Tagami, Y. *J. Chem. Phys.* **1972**, *56*, 3592.
(19) Nagarajan, R.; Ganesh, K. *Macromolecules* **1989**, *22*, 4312.
(20) Munch, M. R.; Gast, A. P. *Macromolecules* **1988**, *21*, 1360.
(21) Press, W. H.; Flannery, B. P.; Teukolsky, S. A.; Vetterling, W. T. *Numerical Recipes*; Cambridge University Press: New York, 1986; p 294.
(22) Utiyama, H.; Takenaka, K.; Mizumori, M.; Fukuda, M.; Tsunashima, Y.; Kurata, M. *Macromolecules* **1974**, *7*, 515.
(23) Watanabe, H.; Kotaka, T. *Polym. Eng. Rev.* **1984**, *4*, 73.
(24) Yamakawa, H. *Modern Theory of Polymer Solutions*; Harper and Row: New York, 1971; p 13.


**Registry No.** (PVP)(PS)(PVP) (block copolymer), 108614-86-4; toluene, 108-88-3.